Research article **Open Access**

Nikolina Nekić, Jordi Sancho-Parramon, Ivančica Bogdanović-Radović, Jörg Grenzer, René Hübner, Sigrid Bernstorff, Mile Ivanda and Maja Buljan*

Ge/Si core/shell quantum dots in alumina: tuning the optical absorption by the core and shell size

DOI 10.1515/nanoph-2016-0133
Received August 2, 2016; revised October 28, 2016; accepted November 29, 2016

Abstract: Ge/Si core/shell quantum dots (QDs) recently received extensive attention due to their specific properties induced by the confinement effects of the core and shell structure. They have a type II confinement resulting in spatially separated charge carriers, the electronic structure strongly dependent on the core and shell size. Herein, the experimental realization of Ge/Si core/shell QDs with strongly tunable optical properties is demonstrated. QDs embedded in an amorphous alumina glass matrix are produced by simple magnetron sputtering deposition. In addition, they are regularly arranged within the matrix due to their self-assembled growth regime. QDs with different Ge core and Si shell sizes are made. These core/shell structures have a significantly stronger absorption compared to pure Ge QDs and a highly tunable absorption peak dependent on the size of the core and shell. The optical properties are in agreement with recent theoretical predictions showing the dramatic influence of the shell size on optical gap, resulting in 0.7 eV blue shift for only 0.4 nm decrease at the shell thickness. Therefore, these materials are very promising for light-harvesting applications.

Keywords: Ge/Si core/shell quantum dots; quantum confinement; absorption; self-assembly.

***Corresponding author: Maja Buljan,** Ruđer Bošković Institute, Bijenička cesta 54, 10 000 Zagreb, Croatia,
e-mail: maja.buljan@irb.hr
Nikolina Nekić, Jordi Sancho-Parramon, Ivančica Bogdanović-Radović and Mile Ivanda: Ruđer Bošković Institute, Bijenička cesta 54, 10000 Zagreb, Croatia
Jörg Grenzer and René Hübner: Helmholtz-Zentrum Dresden-Rossendorf, 01328 Dresden, Germany
Sigrid Bernstorff: Elettra Sincrotrone Trieste, 34149 Basovizza, Italy

1 Introduction

Semiconductor core/shell quantum dots (QDs) receive strong attention due to the tunability of their electronic properties, leading to many relevant nanotechnology and optoelectronic applications [1–7]. Both germanium and silicon are materials frequently used in the electronic industry; in addition, they show strong confinement effects in QDs [7, 8]. Theoretical studies show that Ge/Si core/shell QDs should have significantly different properties than single-material QDs [9]. They have a type II band alignment, causing the holes to localize in the core and the electrons in the shell. As a result, free charge carriers are separated and the exciton lifetime is extended, because the shell acts as a tunneling barrier for the core-localized hole [9–12]. The very recent calculations show that the effective band-gap and exciton binding energy are strongly dependent on the size of the core and shell [12, 13]. Our recent studies demonstrated the possibility to produce Ge/Si core/shell QDs [14]. It is also shown that these materials indeed have specific absorption properties that significantly differ from the absorption of either Ge or Si QDs. However, a detailed investigation of this system as a function of the core/shell QD structure and the confinement effects are still unknown.

Herein, the experimental realization of Ge/Si core/shell QDs embedded in an amorphous alumina matrix with different core and shell sizes is presented, and the quantum confinement effects are investigated. QDs are ordered in a 3D QD lattice within the matrix, and the material is produced by magnetron sputtering deposition. The influence of the core and shell size on the material optical properties and the fabrication conditions of well-ordered Ge/Si QD lattices are studied. A strong dependence of the optical absorption on the core and shell size is demonstrated in accordance with theoretical predictions. Considerably larger band-gap shifts are achieved when compared to pure Ge QDs.

2 Results

2.1 Structural properties

The material structure consists of Ge/Si core/shell QDs that are regularly ordered within the alumina matrix. To fabricate such materials, specific deposition conditions have to be used that ensure the self-ordered growth of QDs and the realization of their core/shell internal structure. To achieve both desired properties, the experience in producing 3D ordered Ge QDs in an Al_2O_3 matrix by Ge/Al_2O_3 multilayer deposition is used [15, 16]. Because Ge QDs form during Ge layer deposition, adding Si in the deposition sequence results in covering the Ge QDs with Si and forming a shell. The scheme of the deposition is shown in Figure 1, whereas the details are given in Section 5. During deposition, Ge QDs form by diffusion-assisted nucleation in the growing layer, whereas the Si layer forms an asymmetric shell around the Ge core.

We have produced two series of samples differing by the size of the Si shell and Ge core. In the first series, the samples are named Ge, Ge/Si1, Ge/Si2, and Ge/Si3 in which the Ge sample has no shell and the shell size in other samples increases. The second series consists of samples Ge1/Si, Ge2/Si, Ge3/Si, and Ge4/Si in which the core size increases and the shell remains constant. To vary the sizes of the core and shell, different deposition times are used. The deposition parameters are given in Table 1. The self-ordered growth regime results in a regular spatial distribution of QDs in the matrix as well as in QD size uniformity [17]. QDs are amorphous after deposition.

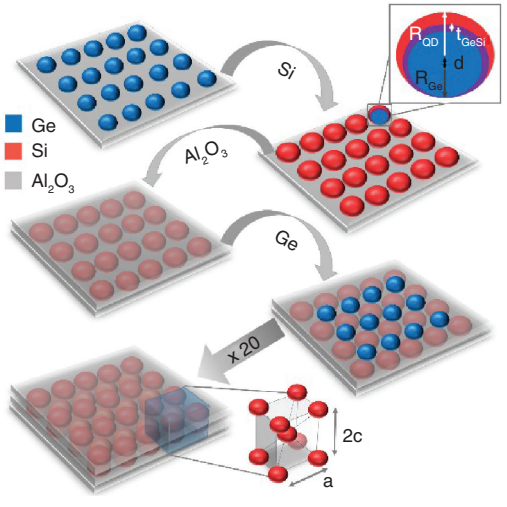

Figure 1: Magnetron sputtering deposition of Al_2O_3/Ge/Si multilayer results in a core/shell QD structure.
The top right inset shows a cross-section of one QD. The core center is shifted and there is an intermixing layer at the interface between Ge and Si.

Table 1: Ge and Si deposition times and atomic percentages for all samples.

Sample	t_{Ge} (s)	t_{Si} (s)	Ge (at.%)	Si (at.%)	Al (at.%)	O (at.%)
Ge	55	0	9.9±0.6	0.82±0.08	27±1	57±3
Ge/Si1	55	30	8.6±0.6	6.5±0.5	27±1	52±3
Ge/Si2	55	60	8.7±0.6	11.3±0.7	26±1	48±3
Ge/Si3	55	90	8.2±0.5	16.2±1	26±1	43±2
Ge1/Si	55	60	8.7±0.6	11.3±0.7	26±1	48±3
Ge2/Si	75	60	12.0±0.8	12.0±0.8	27±1	44±2
Ge3/Si	95	60	13.0±0.7	13.2±0.7	24±1	46±2
Ge4/Si	115	60	16.8±1.1	11.4±0.8	23±1	43±2

The silicon percentage is increasing from samples Ge/Si1 to Ge/Si3, as silicon deposition time is increased. Samples Ge1/Si to Ge4/Si show an increasing percentage of germanium in accordance with the increase in deposition time of germanium.

The typical structure of the films is visible in Figure 2, where cross-sectional transmission electron microscopy (TEM) images of samples Ge/Si3 and Ge4/Si are shown. Both the multilayer structure and the indication of QD ordering are visible for the Ge/Si3 sample. Due to the very small QD size, their complex inner structure, and the fact that a TEM micrograph is a 2D projection of the analyzed sample, it is extremely challenging to distinguish between the core and shell of QDs in TEM images.

A more detailed structural analysis of the films was performed using the grazing incidence small-angle X-ray scattering (GISAXS) method, as it was shown to be very sensitive to the internal structure of core/shell QDs as well as to their arrangement properties [17, 18].

Because of the very small sizes and almost a few atoms thick shells, the core/shell structure is extremely hard to see with TEM measurements. This is why the GISAXS method is very important and interesting. To highlight the sensitivity of this method, the form factors of the core/shell and only core QDs with the same size and arrangement are shown (Figure 3). These images also show how GISAXS maps would look like for a completely disordered system, because the structure factor is then constant. On the contrary, in an ordered system, both the structure and the form factor give a contribution to the final GISAXS map. The results clearly show a difference between the core/shell and core self-assembled QDs, even for very thin shells, thus giving us the powerful tool for core/shell structure investigation.

GISAXS maps of all samples are shown in Figure 4. All maps have four characteristic lateral intensity maxima (Bragg spots) showing that the formed QDs are well

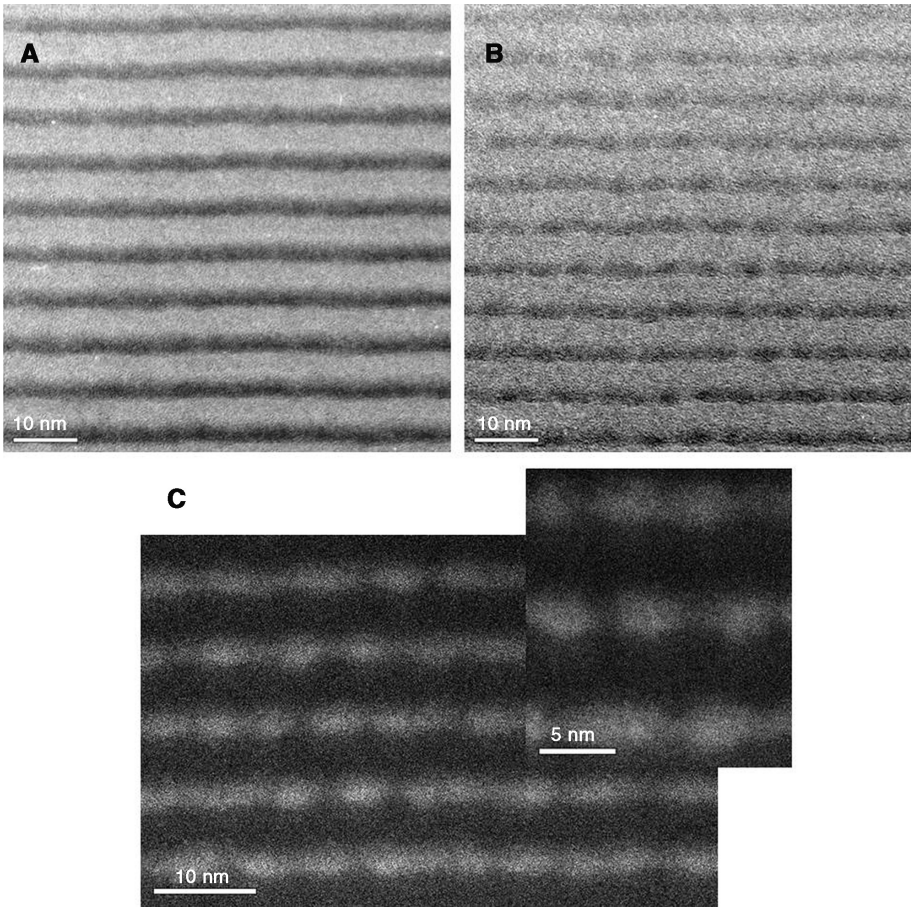

Figure 2: Cross-sectional TEM image of (A) Ge4/Si sample and (B) Ge/Si3 sample and (C) STEM of Ge/Si3 clearly showing QDs of about 3 nm radius.

arranged in a 3D QD lattice. To get the structural parameters, GISAXS maps were numerically analyzed using the model described in Ref. [18]. For the analysis, it was assumed that QDs are arranged in a 3D paracrystal body centered tetragonal (BCT) lattice and that they have a core/shell internal structure, with the center of the core shifted from the shell center (see Figures 1 and 3). It was shown that this model was necessary for a reliable interpretation of GISAXS intensity distributions [14]. The corresponding simulations obtained by numerical analysis are shown in the insets of Figure 4. These simulations are in good agreement with the measurements for $|Q_y| > 0.5\ \mathrm{nm}^{-1}$. For these Q_y-values, the dominant contribution to GISAXS intensities comes from QDs, whereas for the values below there is a significant contribution from the correlated roughness of the multilayer. That contribution is partially responsible for the horizontal sheets appearing in the central part of the GISAXS map. As this contribution is not taken into account in the model used for the description of QDs and the model assumes a 3D lattice of QDs, the central parts of the simulated and experimental maps significantly differ. More details about the appearance of crossings in the simulated maps can be found in Ref. [18]. Because we are interested only in QD information, the mentioned range with the small Q_y values is not important for this study.

The parameters of the analysis are presented in Table 2. From the parameters, it can be seen that the size of the Ge core and Si shell indeed increases as predicted by the deposition parameters. Values of the radius standard deviation σ_R are in the interval [0.2–0.4], where the deviation is higher for the larger radius. The intermixing layer thickness t_{GeSi} for all samples is 0.3 ± 0.1 nm, except Ge/Si1 that has 0.2 ± 0.1 nm thickness. Most of the samples have indeed a very good regular ordering, as confirmed by relatively strong and narrow lateral Bragg spots in GISAXS maps. Only the Ge4/Si sample with the largest core size shows a decreased ordering quality, which is in agreement with TEM results (Figure 2A). As visible in Figure 2A, QDs have merged into a thin layer. Therefore, this sample is left out of further analysis.

The chemical composition of the thin films [i.e. atomic percentages of Ge, Si, Al, and O, measured by

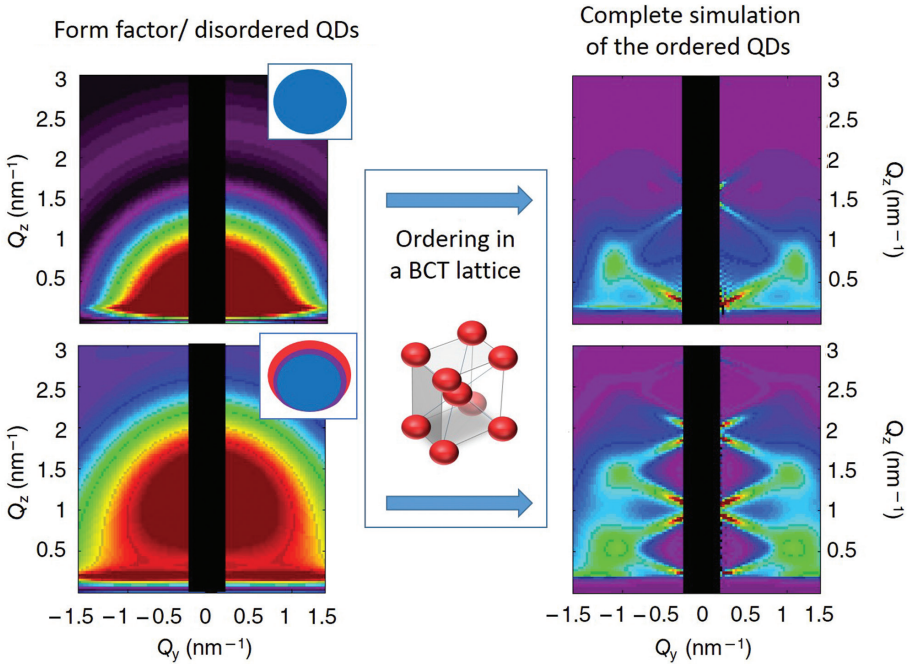

Figure 3: Simulations of GISAXS maps for simple (just core) and core/shell QDs having fully disordered and BCT regular arrangement. For a completely disordered QD system (left column), the structure factor is constant and GISAXS maps are dominated by the form factor contribution only. By ordering QDs in a BCT lattice (right column), there is a contribution from both the structure and the form factor, resulting in the simulations shown in the right side of the figure. A clearly different image for the core/shell and only core QDs of the same size is shown, thus giving us the powerful tool of showing that a core/shell structure is obtained.

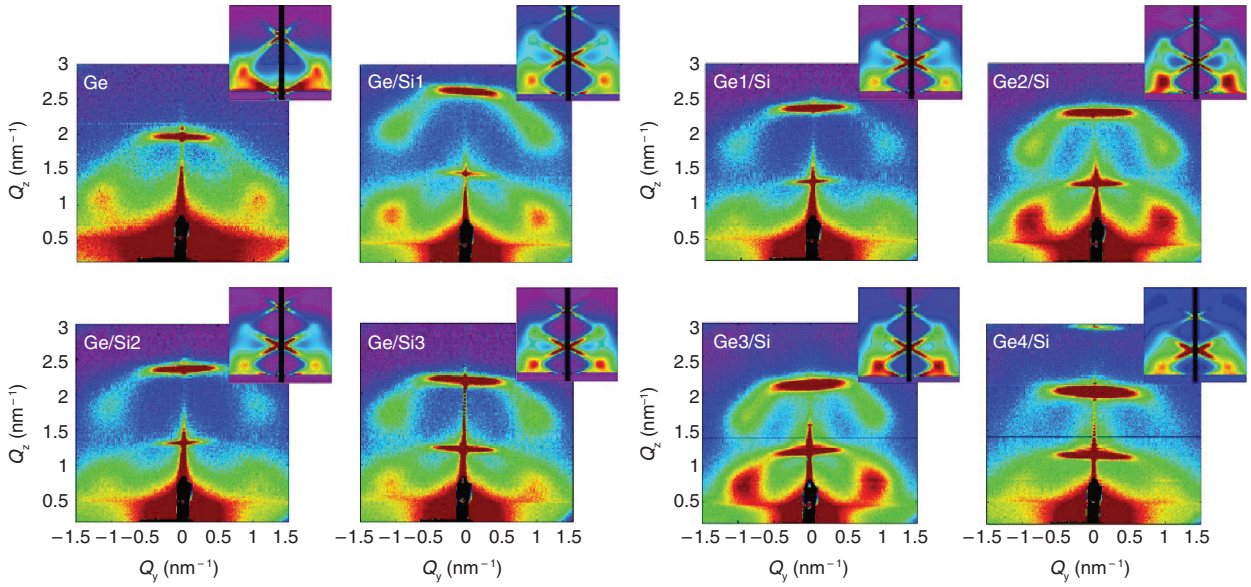

Figure 4: GISAXS maps of all studied samples.
Insets show simulations obtained using the model that was explained in detail elsewhere [18].

time-of-flight electron recoil analysis (ToF-ERDA)], are presented in Table 1. These data are important for checking the amount of Ge and Si contained in QDs and the reliability of the model used for the description of the QD internal structure. From the data, it follows that the percentage of Si is increasing from Ge/Si1 to Ge/Si3, and the atomic percentage of Ge is gradually growing from the Ge1/Si to the Ge4/Si sample in accordance with the deposition

Table 2: QD size determined from GISAXS.

Sample	a (nm)	c (nm)	R_{QD} (nm)	R_{core} (nm)	t_{shell} (nm)	d (nm)
Ge	4.8±0.2	4.1±0.2	1.8±0.2	1.8±0.2	0	0
Ge/Si1	4.9±0.2	5.1±0.2	2.1±0.1	1.70±0.05	0.6±0.2	0.4±0.06
Ge/Si2	4.8±0.2	6.4±0.2	2.4±0.2	1.70±0.05	1.0±0.2	0.6±0.06
Ge/Si3	5.6±0.2	6.8±0.2	2.6±0.2	1.70±0.05	1.3±0.4	0.9±0.06
Ge1/Si	4.8±0.2	6.4±0.2	2.4±0.2	1.70±0.05	1.0±0.2	0.6±0.06
Ge2/Si	6.0±0.2	6.4.±0.1	2.9±0.2	2.2±0.1	1.0±0.5	0.7±0.06
Ge3/Si	6.0±0.2	6.9±0.1	3.0±0.2	2.4±0.1	0.9±0.5	0.6±0.07

QD in-layer separation a, multilayer period c, QD and core radius, shell thickness, and shift of the core center d.

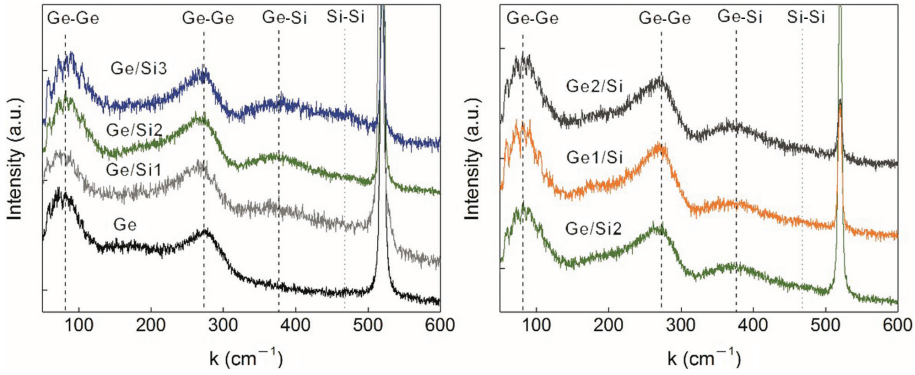

Figure 5: Raman spectrum of Ge, Ge/Si1, Ge/Si2, and Ge/Si3 and Ge1/Si, Ge2/Si, and Ge3/Si samples.

parameters. The results of GISAXS analysis (core and shell size and QD arrangement) were compared to the results of the atomic composition. Using the structural parameters obtained from GISAXS analysis (Table 2), the atomic composition of the crystalline Ge/Si QDs in alumina matrix was calculated. The obtained values agree very well with the values measured by ERDA (Table 1), indicating that GISAXS parameters are reliable.

Raman measurements have been performed to get an insight in the Ge-Ge, Si-Si, and especially Ge-Si bonding properties. The results are summarized in Figure 5. The amorphous Ge-related band appears close to 80 and 275 cm^{-1}, the Ge-Si band appears close to 380 cm^{-1}, and the amorphous Si peak is visible at around 470 cm^{-1}. Raman spectra of the first series of materials (constant Ge-core) clearly show an increase of the Si-related band, whereas the width and intensity of Ge-related bands are nearly constant. The opposite trend is visible for the second series; the intensity of the Ge peak is increasing and becomes narrower as expected for an increase in Ge core size. The Ge-Si band is visible for all samples containing core/shell QDs. It has a nearly constant intensity for all samples, indicating the same thickness of the Ge/Si interface layer, in correspondence with the parameters obtained from GISAXS analysis (Table 2). The exception is the Ge/Si1 sample with the thinnest Si shell, which has a slightly smaller Ge-Si band. This could be simply due to the fact that the Si shell is much thinner, so it only partially covers the mixing layer, and is partially bound to the alumina matrix causing a reduced intensity of the Ge-Si Raman band.

2.2 Optical properties

Ellipsometric analysis was carried out by considering each multilayer structure as a single homogenous film with a thickness equal to the total multilayer thickness and effective optical constants modeled using a flexible multiple-oscillator model [14]. Taking into account that the Al_2O_3 matrix is transparent in the considered spectral range, all the absorption was associated with the presence of Ge/Si QDs. Figure 6 shows the imaginary part of the dielectric function (ε_2) in relation to the size of Si shell (Figure 6, left) and Ge core (Figure 6, right). As visible in Figure 6, Ge/Si QDs present much stronger absorption than Ge QDs. This has been theoretically predicted by the larger dipole transition moments taking place in core/shell QDs in comparison to homogeneous (either Si or Ge) QDs [9]. Ge/Si QDs show a double-peak structure that has

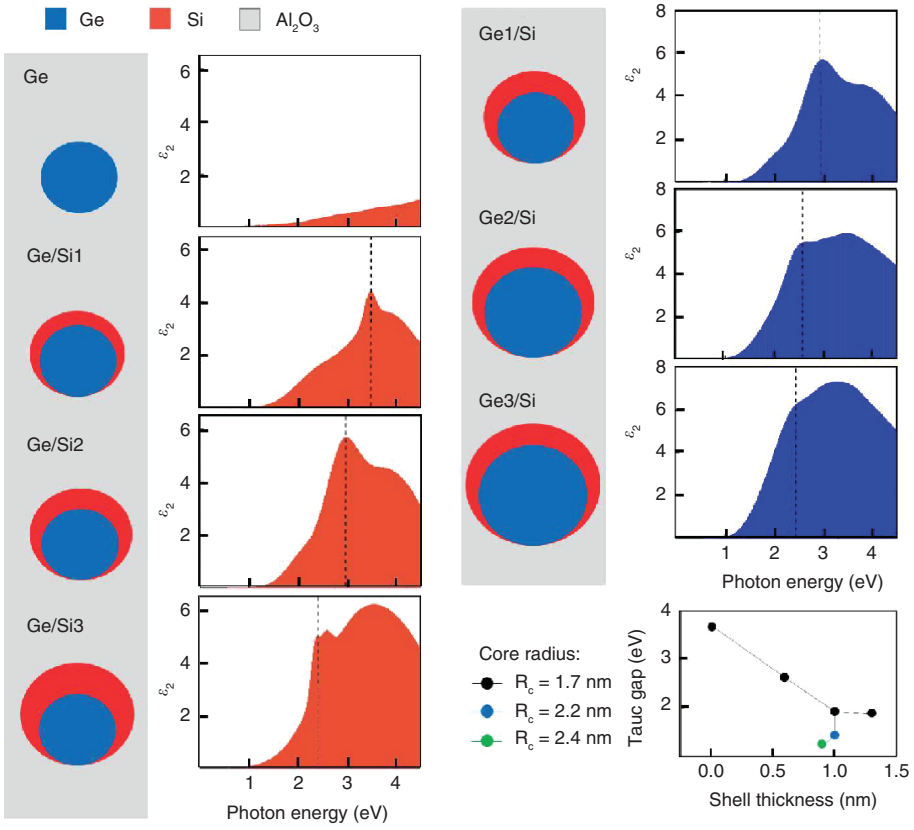

Figure 6: Tuning the optical properties (imaginary part of the dielectric function) by changing the shell thickness (red) and core size (blue). Pure Ge QDs have a lower absorption than Ge/Si QDs. The last image represents the Tauc gap depending on the shell thickness (black dots) and core size (blue and green dots).

been predicted by density functional theory calculations [12]. A strong narrow peak is superimposed on the broad one. Both peaks show a dependence on the size of the core and shell. Remarkable confinement effects are revealed by the evolution of the narrow peak with QD morphology: decreasing the Ge core or Si shell thickness results in a blue shift of the peaks.

Absorption spectra and a Tauc plot for indirect allowed transitions were used to calculate the optical energy gap, often referred to as the Tauc gap [19]. The results are shown in the last inset of Figure 6. The relatively large shifts are obtained for a very small change in the Si shell thickness: the optical band-gap shifts for 0.7 eV when the Si shell increases for only 0.4 nm. That is, a strong dependence of the gap on the Si shell size is visible there.

3 Discussion

Two series of samples were tested and the detailed characterization of the Ge/Si core/shell QD ordering and size properties was performed. The aim was to obtain a spatially ordered array of Ge/Si core/shell QDs in the matrix, because a more regular ordering is related to a narrower size distribution, which is important for the applicability of the material. GISAXS and TEM analyses showed that the self-assembled growth regime can be achieved for core/shell nanostructures up to a limit where QDs are not separated by the matrix any more (i.e. form an almost continuous layer). The self-assembly mechanism is shown to work well for small and also for large Ge cores. The quality of ordering is as good as for the corresponding pure Ge QDs. A great advantage of the Ge/Si core/shell system is the suppression of Ge oxidation by the deposition of Si shell over the Ge. It is well known that Ge oxidates easily, which reduces drastically its emission properties and therefore its potential application [20, 21]. A detailed analysis of Ge oxidation using X-ray fluorescence measurements was carried out (not shown here). A practically complete reduction of Ge oxidation in core/shell QDs was found. Finally, Ge/Si core/shell materials are more stable at higher temperatures. Ge QDs in alumina disintegrate at temperatures above 700°C, whereas in the core/shell system this limit is shifted to values above 800°C [14].

Optical properties, especially absorption, are important for potential solar cell materials. Because of the quantum confinement effect, it is possible to tune the band gap of the nanocrystals. Over the years, this was done for various QD materials [22–24], confirming that there is a red shift in absorption for larger dots. However, core/shell structures are more complex. Specifically, Ge/Si core/shell QDs have a type II band alignment, meaning that electrons and holes are located in different materials, resulting in longer exciton lifetime and smaller recombination probability. The theory predicts a dramatic influence of the core and shell sizes on the optical band-gap [13], which makes these materials very promising for photovoltaic and photodetector applications. Furthermore, there is a significant increase in absorption compared to single-material QDs of the same size and similar arrangement properties [9]. Our data strongly support these theoretical calculations. Pure Ge QDs already have strong quantum confinement effects: a band-gap shift of 0.7 eV was achieved by a Ge radius increase of 1 nm [16]. Adding a Si shell results in an even stronger effect. We show that the band gap reduces for 0.7 eV when the Si shell increases for only 0.4 nm. The core-size dependence is slightly less sensitive; however, it is important that the entire Sun spectrum can be covered by a corresponding tuning of the core- and shell-size properties. The absorption is also significantly increased compared to single-material QDs (Figure 6).

Consequently, these materials are very promising for various optoelectronic applications. They contain all important properties including regular ordering, size homogeneity, tunable band-gap, charge separation, and internal core/shell structure.

4 Conclusion

We have demonstrated the conditions for simple fabrication of 3D regularly ordered Ge/Si core/shell QDs in alumina matrix with highly tunable optical absorption properties. The regimes of the self-assembled growth were explored and it was shown that it occurs in a large range of structural parameters up until the neighboring QDs merge. The optical properties of these materials as well as their dependence on the size of Ge core and Si shell were presented. A very strong dependence of the optical band-gap on the Si shell size was demonstrated. The observed optical features were in agreement with the most recent theoretical predictions.

5 Experimental section

The investigated samples were produced by magnetron sputtering deposition using a KJLC CMS-18 system. The deposition conditions were chosen to ensure the self-assembled growth of QDs and their internal core/shell structure [14]. The thin films were deposited on glass and Si(100) substrates at the temperature of 300°C. Seven samples were investigated and separated into two groups: in the first group (Ge, Ge/Si1, Ge/Si2, and Ge/Si3), the thickness of the shell was varied; in the second group (Ge1/Si, Ge2/Si, Ge3/Si, and Ge4/Si), the core size was changed, but the amount of Si remained the same. For systematical reasons, the Ge/Si2 sample was also named Ge1/Si. Because of the specific core and shell sizes, this sample can be classified into both groups. The deposition parameters for all samples, including deposition times for Ge, Si, and Al_2O_3, are summarized in Table 1. The Ar pressure during deposition was 0.47 Pa, whereas the sputtering powers were 10, 50, and 300 W for Ge, Si, and Al_2O_3, respectively.

The ordering of QDs as well as the core and shell sizes depending on the deposition parameters were investigated using the GISAXS method. These measurements were performed at the synchrotron Elettra, Trieste, at the SAXS beamline, using a photon energy of 8 keV and a 2D photon detector. Some selected samples were analyzed using TEM employing an image C_s-corrected Titan 80–300 (FEI) microscope operated at an acceleration voltage of 300 kV. Besides cross-sectional bright-field TEM micrographs, atomic number contrast images were recorded in high-angle annular dark-field scanning TEM mode (HAADF-STEM). The atomic composition of the films was determined by ToF-ERDA, whereas Ge and Si bonding was explored by Raman spectroscopy (DILOR Z-24 triple monochromator and an argon ion laser with an excitation line at 514.5 nm). The optical properties were investigated using ellipsometry with a VASE ellipsometer from J.A. Wollam Co, Inc., in the spectral range between 1 and 5 eV and incidence angles of 65°, 70°, and 75°.

Acknowledgments: The authors are grateful to Joško Erceg and Marko Jerčinović for the help in the sample preparation. N.N. and M.B. acknowledge the Croatian Science Foundation (pr.no. 2334), which supported this investigation. Support by the Croatian Centre of Excellence for Advanced Materials and Sensing devices as well as by the Ion Beam Center (IBC) at HZDR is gratefully acknowledged.

References

[1] Kechiantz A, Afanasev A, Lazzari JL. Impact of spatial separation of type-II GaSb quantum dots from the depletion region on the conversion efficiency limit of GaAs solar cells. Prog Photovolt Res Appl 2015;23:1003–16.

[2] Kong EH, Chang YJ, Park HJ, Jang HM. Bandgap tuning by using a lattice distortion induced by two symmetries that coexist in a quantum dot. Small 2014;10:1300–7.

[3] Zhu H, Song N, Lian T. Wave function engineering for ultrafast charge separation and slow charge recombination in type II core/shell quantum dots. J Am Chem Soc 2011;133:22.

[4] Fölsch S, Martinez-Blanco J, Yang J, Kanisawa K, Erwin SC. Quantum dots with single-atom precision. Nat Nanotechnol 2014;9:505–8.

[5] Bao J, Bawendi MG. Nanotechnology: colourful particles for spectrometry. Nature 2015;523:39–40.

[6] Ossicini S, Amato M, Guerra R, Palummo M, Pulci O. Silicon and germanium nanostructures for photovoltaic applications: ab initio results. Nanoscale Res Lett 2010;5:1637–49.

[7] Palummo M, Onida G, Del Sole R. Optical properties of germanium nanocrystals. Phys Stat Sol 1999;175:23–31.

[8] Bensahel D, Canham LT, Ossicini S. Optical properties of low dimensional silicon structures. Dordrecht, Amsterdam: Kluwer, 1993.

[9] Oliveira EL, Albuquerque EL, de Sousa JS, Peeters FM, Farias GA. Configuration-interaction excitonic absorption in small Si/Ge and Ge/Si core/shell nanocrystals. J Phys Chem C 2012;116:4399–407.

[10] Shik A, Ruda H, Sargent EH. Non-equilibrium carriers and recombination phenomena in type-II quantum dots. Nanotechnology 2001;12:523–8.

[11] Ramos LE, Furthmuller J, Bechstedt F. Quantum confinement in Si- and Ge-capped nanocrystallites. Phys Rev B 2005;72:045351.

[12] Javan MB. Ge-Si and Si-Ge core-shell nanocrystals: theoretical study. Thin Solid Films 2015;589:120–4.

[13] Nestoklon MO, Poddubny AN, Voisin P, Dohnalova K. Tuning optical properties of Ge nanocrystals by Si shell. Available from: http://arxiv.org/abs/1605.08610.

[14] Buljan M, Radić N, Sancho-Paramon J, et al. Production of three-dimensional quantum dot lattice of Ge/Si core-shell quantum dots and Si/Ge layers in an alumina glass matrix. Nanotechnology 2015;26:065602.

[15] Buljan M, Jerčinović M, Siketić Z, et al. Growth of a three-dimensional anisotropic lattice of Ge quantum dots in an amorphous alumina matrix. J Appl Cryst 2003;46:1490–500.

[16] Buljan M, Radić N, Ivanda M, et al. Ge quantum dot lattices in Al_2O_3 multilayers. J Nanopart Res 2013;15:1485–98.

[17] Buljan M, Desnica UV, Dražić G, et al. Formation of three-dimensional quantum-dot superlattices in amorphous systems: experiments and Monte Carlo simulations. Phys Rev B 2009;79:035310.

[18] Buljan M, Radić N, Bernstorff S, Dražić G, Bogdanović-Radović I, Holý V. Grazing-incidence small-angle X-ray scattering: application to the study of quantum dot lattices. Acta Cryst A 2012;68:124–38.

[19] Tauc J, Grigorovici R, Vancu A. Optical properties and electronic structure of amorphous germanium. Phys Stat Sol 1996;15:628–37.

[20] Liu H, Winkenwerder W, Liu Y, et al. Core-shell germanium-silicon nanocrystal floating gate for nonvolatile memory application. IEEE Trans Electron Devices 2008;55:3610–4.

[21] Cosentino S, Mirabella S, Miritello M, et al. The role of the surfaces in the photon absorption in Ge nanoclusters embedded in silica. Nanoscale Res Lett 2011;6:135.

[22] Lei D, Shen YT, Feng YY, Feng W. Recent progress in the fields of tuning the band gap of quantum dots. Sci China Technol Sci 2012;55:903–912.

[23] Norris DJ. Measurement and assignment of the size-dependent optical spectrum in cadmium selenide (CdSe) quantum dots. Ph.D. thesis. MIT, 1995.

[24] Consentino S, Barbagiovanni EG, Crupi I, et al. Size dependent light absorption modulation and enhanced carrier transport in germanium quantum dots devices. Solar Energy Mater Solar Cells 2015;135:22–8.